European Journal of Molecular & Clinical Medicine
ISSN 2515-8260 Volume 07, Issue 07, 2020

Fabrication And Characterization Of Strontium Ferrite Prepared Through Precursor Route.

Jashanpreet Singh

Department of Chemistry, Lovely Professional University, Phagwara-144001

Email: jashanpreet.21529@lpu.co.in

Abstract

Strontium ferrite nanoparticles were synthesized in the presence of strontium ferricarboxylate precursor by using thermolysis precursor route. Simultaneous Thermogravimetry-Differential Scanning Calorimetry was used to study and analyze the thermolysis process. X-ray diffraction study reveals the formation homogenous spinel type cubic structure of the strontium ferrite nanoparticles. A reaction pathway was identified from the thermal decomposition of strontium hexapropionato ferrate(III) precursor to the final product. Mössbauer parameters were analyzed for the precursor, intermediates, final product and compared with the literature reported values.

Introduction

Ferrite nanoparticles are called magnetic nanoparticles and have received a considerable amount of attention due to their wide applications in various fields, ranging from biomedical via electronics towards industrial [1-5]. These are considered as metal oxides that are categorized commonly in the spinels with general formula AB_2O_4, in which A and B are the metal cations placed at the crystallographic sites known as tetrahedral (A site) and octahedral (B site). The cations placed in these crystallographic symmetries are tetrahedrally and octahedrally bonded to oxygen atoms. Depending upon the distribution of cations, they exhibit different properties such as magnetic, dielectric and optical. Further, irrespective of their spinel structure, ferrite nanoparticles show a wide range of applications such as catalyst, waste water treatments, ferrofluids, and electronic devices [6-8], each application requires ferrites to display different properties.

In recent decades, pure alkali, transition and mixed metal ferrite nanoparticles have gained a lot of attention after the literature survey. Nanosized lithium ferrites have displayed exceptional magnetic properties that makes them promising candidate to be used as contracting agents in magnetic resonance imaging, as magnetic carriers in biomedical applications [9]. Similarly, transition metal ferrite nanoparticles such as Mn^{2+}, Fe^{2+}, Co^{2+}, Ni^{2+}, Cu^{2+}, and Zn^{2+} have been reported by many scientists with wide range of applications such as photo-catalytic degradation, magnetic cores in transformers and generators, depending upon the properties varying from high magnetic permeability, low cost to high temperature stability [10-11].

Researchers have published various articles showing many ferrite nanoparticles with different synthetic methods. Methods used for preparing the ferrites are co-precipitation, hydrothermal,

auto-combustion, sol-gel, sonochemical, microwave assisted, polyol [12-16], out of which four methods mentioned first are the most common ones. These synthetic methods have both advantages as well as disadvantages. Advantages of these techniques are higher yields, milder reaction conditions, improved selectivity but certain disadvantages are crystal defects induced in the final products, high temperature is required, reaction time. Therefore, no method has been reported in the literature with complete advantages only. Keeping in view, we tried to adopt thermal decomposition method to prepare strontium ferrite using its ferri-hexapropionato counterpart. In order perform thermal decomposition, thermal technique such as simultaneous thermogravimetric along with differential thermal analysis has been adopted. The choosing of correct synthetic method plays a critical role for preparing the ferrite nanoparticles with desired properties and displaying the applications.

Materials and Methods

All the chemicals such as strontium nitrate (>99.9 %), ferric chloride (97 %), propionic acid (>99.5 %) were obtained from Sigma Aldrich and were used without further purification. Strontium ferricarboxylate precursor, $Sr_3[Fe(CH_3CH_2COO)_6]_2$ was prepared by mixing solutions of salts of ferric chloride with strontium nitrate in their respective stoichiometry. Solution of carboxylic acid was added dropwise in order to obtain the desired precursor. The obtained solution mixture was stirred and the temperature $60^{\circ}C$ is maintained till it changed into the transparent solution. Further, the obtained solution mixture was heated on water bath in order to obtain the product with brown color. The product was filtered using filter paper, washed with water and at last, kept in vacuum desiccator for overnight.

Thermal analysis was performed using Simultaneous non-isothermal thermograms (TG/DTG/DTA-DSC) were recorded on a Pyris Diamond Model (Perkin Elmer) and SDT Q600 (TA instruments) at a heating rate of $5^{o}C\ min^{-1}$ in flowing air atmosphere. Final strontium ferrite obtained from thermal decomposition was confirmed using Panalytical (PW3064) X-ray diffractometer, Mössbauer spectrometer.

Results and Discussion

Mössbauer spectrum of the as-synthesized precursor (Fig. 1) indicate a doublet with δ values lie between 0.32-0.36 mm/s and Δ values lying between 0.40-0.51 mm/s [17]. The obtained values are attributed to the high spin nature of Fe (III) with octahedral symmetry in which iron is bonded to six propionate ligands through oxygen atom of carboxylate groups.

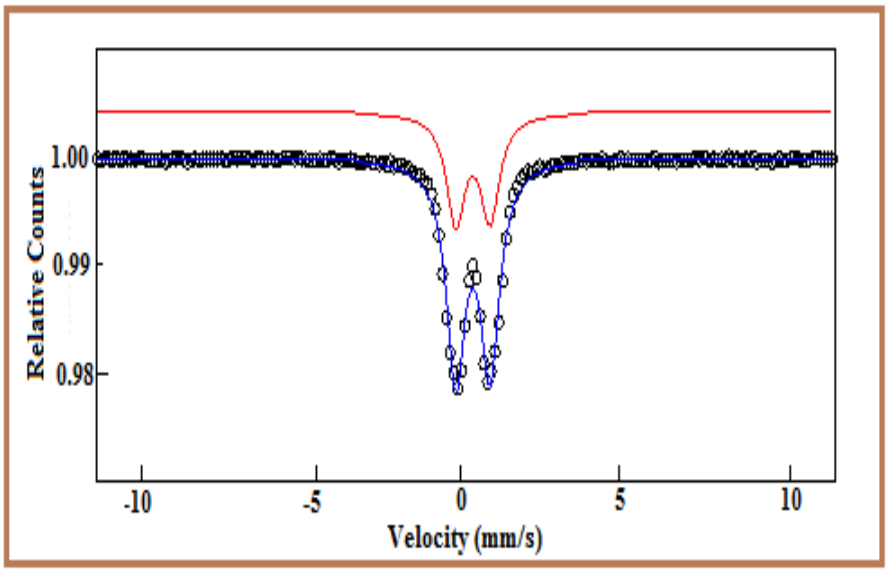

Fig. 1 Mössbauer spectrum of the as-synthesized precursor.

Figure 2 displays the simultaneous thermal curves of strontium hexa (propionato) ferrate(III) precursor in aerial atmosphere with heating rate of 10 °C per min. The precursor remains stable till 360°C of temperature, the dehydrated precursor undergoes an oxidative decay with loss in the weight of 45.66 % around 475°C revealing the formation of Fe_2O_3 and strontium oxalate (calculated weight loss = 45.83%). Corresponding to this step, there exist a DTG peak and a strong exotherm centered at 400°C. The formation of α-Fe_2O_3 has been confirmed by analyzing the Mössbauer spectrum (Figure 3) of the obtained residue by calcining the precursor around 500°C. The central quadrupole doublet is observed that appears due to the nuclei of the ions present on the surface and the effective magnetic field associated with them. Mössbauer parameters (Table 1) are in agreement to those reported for α-Fe_2O_3 particles [13] with average particle size lies between 15-20 nm. At higher temperature (800°C), strontium oxalate decomposes to strontium carbonate. As heating continues, strontium carbonate and α- Fe_2O_3 undergo a reaction above 800°C to form $Sr_2Fe_2O_5$ as supported by a mass loss of 58.16 % (calc. loss= 58.80 %) and an exothermic region in DTA. The left product i.e. $SrCO_3$ in the final thermolysis step was treated with 2N HNO_3 to get the pure final ferrite, $Sr_2Fe_2O_5$, followed by repeated washings with distilled water. Based on the above observations, the proposed reaction pathway of aerial thermolysis for strontium hexa(propionato)ferrate(III) precursor is:

$$Sr_3\,[Fe(CH_3CH_2COO)_6]_2 \xrightarrow{475°C} 3SrC_2O_4 + \alpha\text{-}Fe_2O_3 + \text{gaseous products}$$

$$3SrC_2O_4 \xrightarrow{800°C} 3SrCO_3 + 3CO$$

$$3SrCO_3 + \alpha\text{-}Fe_2O_3 \xrightarrow{>800°C} Sr_2Fe_2O_5 + SrCO_3$$

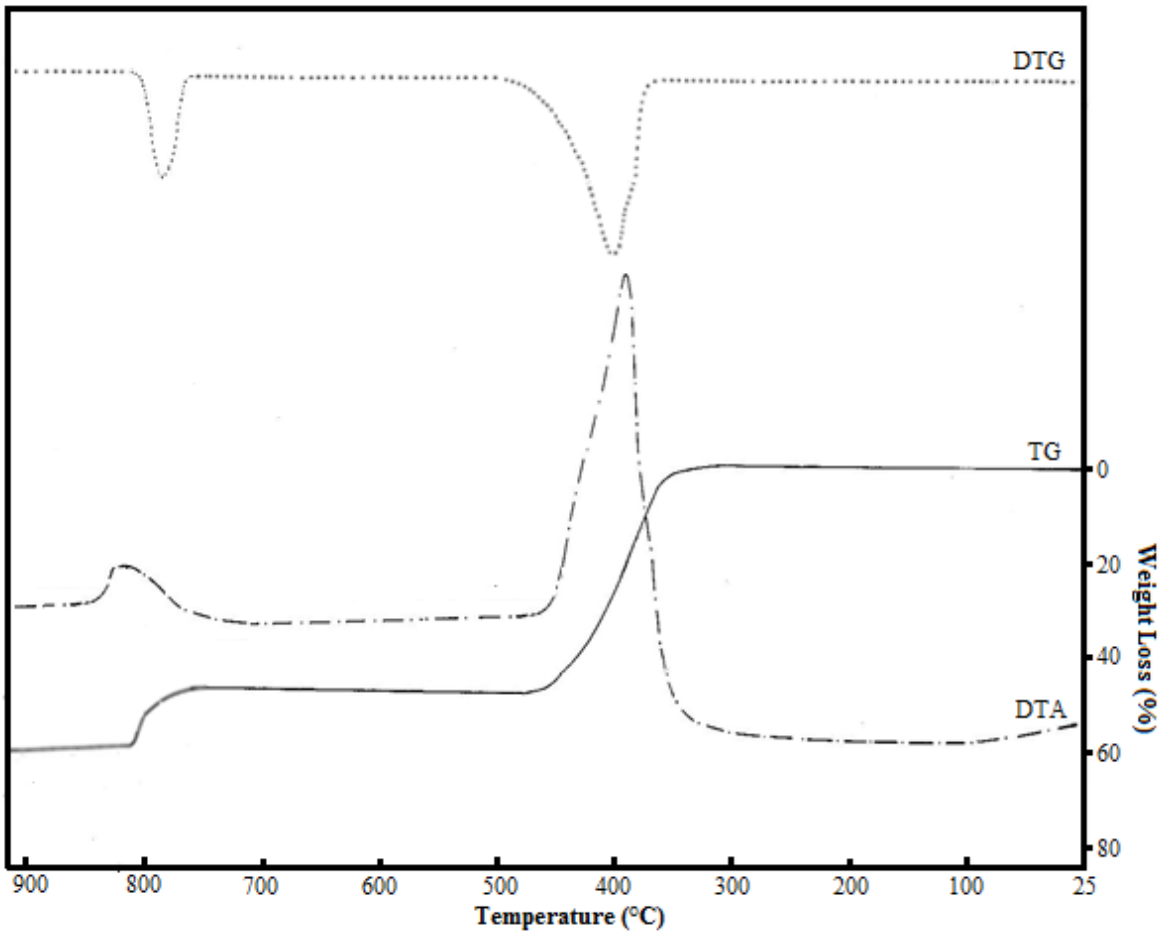

Fig. 2 Thermolysis graph of strontium hexa(propionato) ferrate(III) precursor.

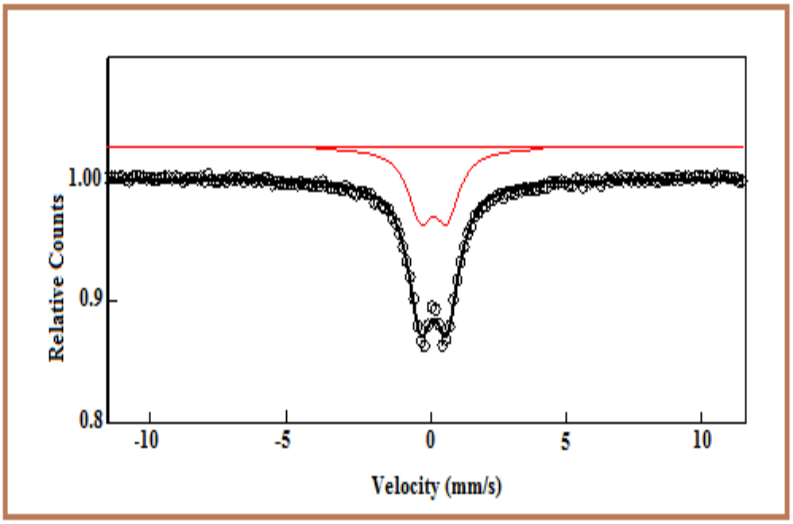

Fig. 3 Room temperature Mössbauer spectrum of the intermediate calcined at 500° C.

Table 1. Mössbauer parameters of the intermediates and final products measured at 300K.

Temp. of Calcination (°C)	δ# (mm/s)	Δ (mm/s)	B* (T)	Cationic (Fe^{3+}) distribution (%)	Assignment
500	0.31	0.76	49.8	-----	α-Fe_2O_3
850	0.28	0.47	48.7	46.5 (oct)	$Sr_2Fe_2O_5$
	0.32	0.39	46.7	35.9 (tet)	
	0.14	0.23	--(CD)	17.6	

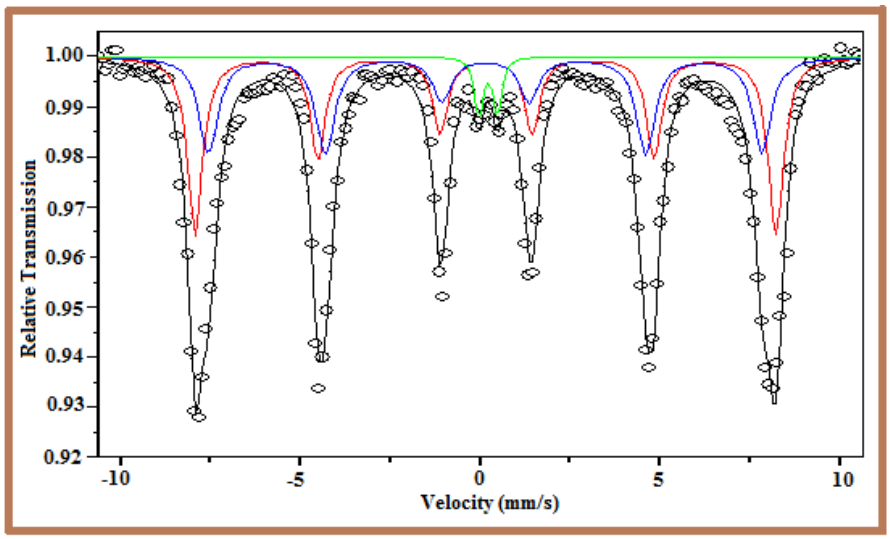

Fig. 4 Room temperature Mössbauer spectrum of strontium ferrite.

The formation of the strontium ferrite has been proved by reporting Mossbauer spectrum (Fig. 4) at room temperature and analyzing Mössbauer parameters. The spectrum consists of two six line patterns super positioned on each other, also known as hyperfine sextets. The peaks seen in the sextet are both intense as well as broad that can be correlated to the nuclei of the inner ions and surface ions respectively of the nanoparticles. In spite of the fact, the latter will most likely contribute towards the sharing of effective magnetic fields and maybe isomer shifts as well as quadrupole splittings to the spectrum, the software fitted Lorentzian curves are sensibly acceptable. From the investigated spectrum, the Mössbauer parameters are deduced and given in Table 1. The shape of the Mössbauer spectrum resemble to that of the reported spectra [19].

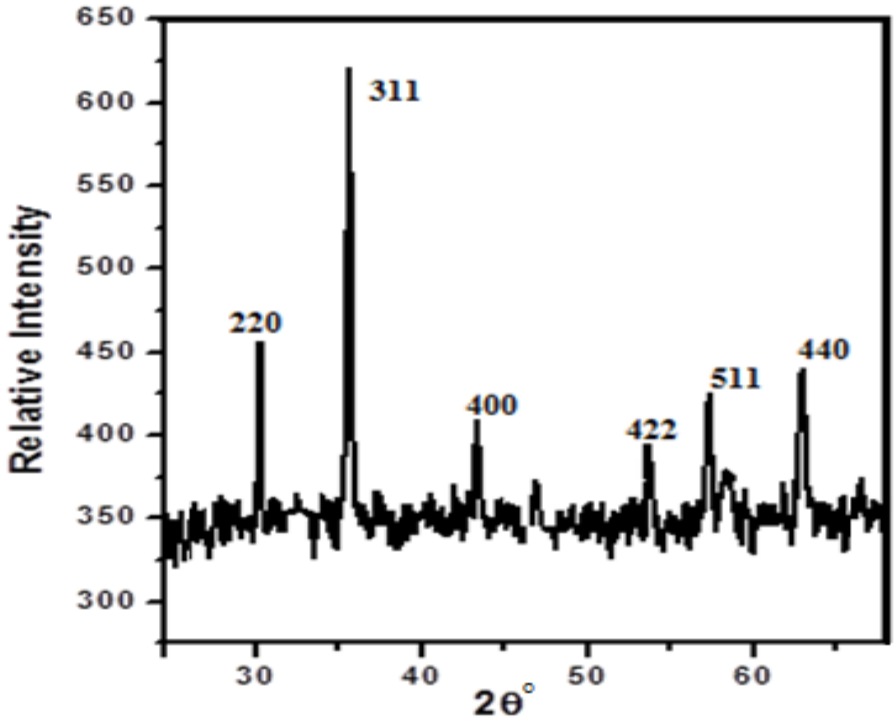

Fig. 5 Powder XRD pattern of the as synthesized strontium ferrite.

Powder XRD pattern (Fig. 5) displays different reflections indexed by respective miller indices (hkl values). All the broad peaks indicates their nanocrystalline nature of the formed ferrite. Further, it also confirmed the spinel type phase of the ferrite with Fd3M space group i.e. cubic structure. Further, the intensity of the prominent reflection peak of cubic and homogenous spinel ferrite at 311 plane can be distinguishable as a proportion of its extent of crystalline nature [20-24].

Conclusion

Thermolysis of strontium hexapropionato(III) ferrate precursor lead to the formation of strontium ferrite, confirmed by simultaneous thermal analysis (TG-DTG-DSC), Mössbauer study and X-ray diffraction powder pattern. The process used proves to be advantageous as compared to the conventional methods, as improved yield of product was obtained with minimal crystal defects. The intermediates obtained during thermal decomposition process was confirmed by Mössbauer parameters and compared with the reported values, were found to be in agreement. X-ray diffraction pattern of strontium ferrite confirms the cubic spinel phase and nanocrystalline nature.

Acknowlegement

The authors are thankful to Lovely Professional University, Phagwara for providing the laboratory and equipments during experiments performed.

References

1. Kefeni, K. K. Msagati, T. A.M. Mamba, B. B. Ferrite nanoparticles: Synthesis, characterisation and applications in electronic device. Materials Science and Engineering B 215 (2017) 37–55.
2. Gupta, V. K., Singh, L. P., Singh, R., Upadhyay, N., Kaur, S. P., & Sethi, B. (2012). A novel copper (II) selective sensor based on dimethyl 4, 4′(o-phenylene) bis (3-thioallophanate) in PVC matrix. *Journal of Molecular Liquids*, *174*, 11-16.
3. Electrochemical performance of zirconia/graphene oxide nanocomposites cathode designed for high power density supercapacitor
4. Mukherjee, R. (2020). Electrical, thermal and elastic properties of methylammonium lead bromide single crystal. Bulletin of Materials Science, *43*(1), 1-5.
5. Mukherjee, R., Lawes, G., & Nadgorny, B. (2014). Enhancement of high dielectric permittivity in CaCu3Ti4O12/RuO2 composites in the vicinity of the percolation threshold. Applied Physics Letters, *105*(7), 072901.
6.Wei, J., Zhang, X., Liu, Q., Li, Z., Liu, L. and Wang, J., Magnetic separation of uranium by $CoFe_2O_4$ hollow spheres. Chemical Engineering Journal, 241 (2014) 228-234.
7. Ibrahim, I., Ali, I.O., Salama, T.M., Bahgat, A.A. and Mohamed, M.M., (2016) Synthesis of magnetically recyclable spinel ferrite (MFe2O4, M= Zn, Co, Mn) nanocrystals engineered by sol gel-hydrothermal technology: High catalytic performances for nitroarenes reduction. Applied Catalysis B: Environmental, *181*, pp.389-402.
8. Qu, X., Brame, J., Li, Q. and Alvarez, P.J., 2013. Nanotechnology for a safe and sustainable water supply: enabling integrated water treatment and reuse. Accounts of Chemical Research, *46*(3), 834-843.
9. Kefeni, K.K., Msagati, T.A., Nkambule, T.T. and Mamba, B.B., 2019. Spinel ferrite nanoparticles and nanocomposites for biomedical applications and their toxicity. *Materials Science and Engineering: C*, 110314.
10. Abraham, A.G., Manikandan, A., Manikandan, E., Vadivel, S., Jaganathan, S.K., Baykal, A. and Renganathan, P.S., 2018. Enhanced magneto-optical and photo-catalytic properties of transition metal cobalt (Co^{2+} ions) doped spinel $MgFe_2O_4$ ferrite nanocomposites. *Journal of Magnetism and Magnetic Materials*, *452*, 380-388.
11. Luo, M., Dujic, D. and Allmeling, J., 2018. Modeling Frequency Independent Hysteresis Effects of Ferrite Core Materials Using Permeance–Capacitance Analogy for System-Level Circuit Simulations. *IEEE Transactions on Power Electronics*, *33*(12), 10055-10070.
12. Tian, Y., Yu, B., Li, X. and Li, K., 2011. Facile solvothermal synthesis of monodisperse Fe 3 O 4 nanocrystals with precise size control of one nanometre as potential MRI contrast agents. *Journal of Materials Chemistry*, *21*(8), pp.2476-2481.
13. Wongpratat, U., Maensiri, S. and Swatsitang, E., 2015. EXAFS study of cations distribution dependence of magnetic properties in Co1− xZnxFe2O4 nanoparticles prepared by hydrothermal method. *Microelectronic Engineering*, *146*, pp.68-75.
14. Masthoff, I.C., Kraken, M., Mauch, D., Menzel, D., Munevar, J.A., Saitovitch, E.B., Litterst, F.J. and Garnweitner, G., 2014. Study of the growth process of magnetic nanoparticles obtained via the non-aqueous sol–gel method. *Journal of materials science*, *49*(14), pp.4705-4714.
15. Flores-Arias, Y., Vázquez-Victorio, G., Ortega-Zempoalteca, R., Acevedo-Salas, U., Ammar, S. and Valenzuela, R., 2015. Magnetic phase transitions in ferrite nanoparticles characterized by electron spin resonance. *Journal of Applied Physics*, *117*(17), 17A503.

16. Mukherjee, R., Huang, Z. F., & Nadgorny, B. (2014). Multiple percolation tunneling staircase in metal-semiconductor nanoparticle composites. Applied Physics Letters, *105*(17), 173104.

17. Vertes A., Korecz L. and Burger K., *Mössbauer Spectroscopy*, Elsevier Sci. Publ. Co., New York (1979).

18. Greenwood N. N. and Gibb T. C., *Mössbauer Spectroscopy*, Chapman and Hall Ltd., London (1971).

19. Van Der Kraan A. M. (1973) Mössbauer Effect Studies of Surface Ions of Ultrafine α-Fe_2O_3 Particles. Phys. Stat. Sol. 18, 215-226.

20. International Centre for Diffraction Data, *X-ray powder diffraction patterns,* ICDD, Newtown Square (1996).

21. Kumar, P., Khatri, T., Bawa, H., & Kaur, J. (2017, July). ZnO-Fe2O3 heterojunction for photocatalytic degradation of victoria blue dye. In *AIP Conference Proceedings* (Vol. 1860, No. 1, p. 020065). AIP Publishing LLC.

22. KUMAR, P., SAMIKSHA, S., & GILL, R. (2018). Carbon Monoxide Gas Sensor Based on Fe-ZnO Thin Film. *Asian Journal of Chemistry*, *30*(12), 2737-2742.

23. Thakur, A., Kumar, A., Kumar, P., Nguyen, V. H., Vo, D. V. N., Singh, H., ... & Kumar, D. (2020). Novel synthesis of advanced Cu capped Cu2O nanoparticles and their photo-catalytic activity for mineralization of aqueous dye molecules. *Materials Letters*, *276*, 128294.

24. Gill, R., Ghosh, S., Sharma, A., Kumar, D., Nguyen, V. H., Vo, D. V. N., ... & Kumar, P. (2020). Vertically aligned ZnO nanorods for photoelectrochemical water splitting application. *Materials Letters*, *277*, 128295.